Construction of a Supramolecular Fluorescence Sensor from Water-soluble Pillar[5]arene and 1-Naphthol for Recognition of Metal Ions

Xin Yi Zhu,[a] Xi Nan Yang,[a] Yang Luo,[a] Carl Redshaw,[b] Ming Liu,[a] Zhu Tao [a] and Xin Xiao*[a]

[a] Ms. X. Y. Zhu, Prof. X. N. Yang, Dr. Y. Luo, Dr. M. Liu, Prof. Z. Tao, Prof X. Xiao
Key Laboratory of Macrocyclic and Supramolecular Chemistry of Guizhou Province, Guizhou University,
E-mail: gyhxxiaoxin@163.com (X. Xiao)
[b] Prof. C. Redshaw
Department of Chemistry, University of Hull, Cottingham Rd, Hull, HU6 7RX, U.K.

Abstract: A new fluorescent chemosensor comprised of a pyridine functionalized pillar[5]arene (PyP5) and 1-naphthol has been designed and utilized for the recognition of metal cations. The 1-naphthol was encapsulated by the PyP5 cavity and formed a 1:1 host - guest inclusion complex. Whilst free 1-naphthol is known to be strongly fluorescent, this strong fluorescence was quenched in the inclusion complex PyP5@1-naphthol. Using the PyP5@1-naphthol inclusion complex as a fluorescent probe, various metal cations have been detected. The experimental results revealed that the probe responded to both Ag^+ and Fe^{3+}, via an obvious fluorescence quenching or an incomplete quenching of fluorescence, respectively. As a result, a fluorescence method for the detection of two metal cations using a single system has been developed.

Introduction

The selective monitoring of metal ions is very significant because they play a crucial role in biological systems and in the environment[1-10]. Iron is the most abundant transition metal in the human body and exists in two biologically related oxidation states: Fe^{2+} and Fe^{3+}. Fe^{3+} is an essential element in the human body[11-14], and is central to hemoglobin, myosin and many cofactors involved in enzyme activity. At the cellular level, it plays a vital role in the exchange of cytochrome and oxygen transport. Excessive Fe^{3+} will have adverse effects on human health and immunity, leading to serious mental illness, hemochromatosis, neurodegenerative diseases and so on[15-18]. However, if the human body is short of Fe^{3+} for a prolonged time, or if the absorption of iron is hindered, it will be difficult for the human body to produce hemoglobin, which can result in reduced hemoglobin levels, and even iron deficiency anemia. At this time, the ability of blood oxygen supply is reduced, the skin color is pale, making people feel tired and weak, affecting the overall physiological function of the human body. Such issues are likely to lead to pancreatic, heart, lung and other functional organ disorders. Some researchers have confirmed that Alzheimer's disease and Parkinson's disease are related to Fe^{3+}. Another metal ion, Ag^+, is also extremely important. Silver is a precious metal that is widely used in photography, imaging, batteries, semiconductors and a number of other industries. Recently, soluble silver compounds and colloidal silver have been used in the treatment of mental illness, epilepsy, nicotine addiction, gastroenteritis, and infectious diseases, because of their antibacterial activity. However, Ag^+ is a heavy metal environmental pollutant, and high concentrations of Ag^+ will accumulate in the body due to food, and this will result in many adverse effects on health, such as brain damage, nerve and immune system damage[19-23]. Therefore, the detection of silver ions is also of great significance[24-28]. However, so far, effective and standardized tests for the characterization of Ag^+ and Fe^{3+} have been limited and are relatively complex. Therefore, it is very important to develop a highly sensitive and selective detection method for Ag^+ and Fe^{3+}. Fluorescence sensors have the advantages of simple operation, high sensitivity, fast detection and real-time detection. Therefore, it is desirable to design a simple, sensitive, and rapid fluorescent detection probe for detecting Ag^+ and Fe^{3+}, which can be employed for practical applications.

First reported in 2008, pillar[*n*]arenes are now receiving more and more attention[29-34]. Amongst the pillar[*n*]arene family, the use of pillar[5]arene has many advantages[35-40]: (1) it binds neutral molecules in organic solvents because it has an electron-rich cavity; (2) it can provide 10 functionalized reaction sites; (3) its structure provides a rigid component for the preparation of functional materials, and has shown great potential in sensors, catalysts, supramolecular gels, separation and storage. Therefore, pillar[5]arene is very suitable for use in host-guest inclusion complexation in order to design a fluorescent probe[41-49].

On the other hand, 1-naphthol is an important intermediate of fine chemicals, which is widely used in the synthesis and production of dyes, spices, oils, medicines and pesticides[50-52]. The oxygen atom of 1-naphthol is sp^2 hybridized and can form extensive π bonds, and can exhibit strong fluorescence. The successful preparation of water-soluble pillar[5]arene can provide new opportunities for chemists working in the field of host–guest chemistry and the recognition of metal ions. Therefore, more and more research has centered on the synthesis of water-soluble pillar[5]arenes[53-56]. On this basis, we have synthesized a pyridine functionalized pillar[5]arene. Pyridine functionalized pillar[5]arenes are extremely soluble in water and strongly bind 1-naphthol in water, which is mainly driven by hydrophobic and electrostatic interactions. The probe system is constructed by encapsulating one equivalent of 1-naphthol, which possess strong intrinsic fluorescence, into the hydrophobic cavity of PyP5. To this inclusion complex, namely PyP5@1-naphthol, were added

metal ions. The addition of Ag^{+} led to incomplete quenching of fluorescence, whilst Fe^{3+} led to complete quenching of fluorescence. Based on the linear relationship between the fluorescence intensity and the concentration of Ag^{+} and Fe^{3+}, a simple fluorescent probe method for the analysis of Ag+ and Fe^{3+} was constructed. The observed visual signals indicate the potential of this probe system in rapid assay applications.

Results and Discussion

Interaction of PyP5 and 1-naphthol

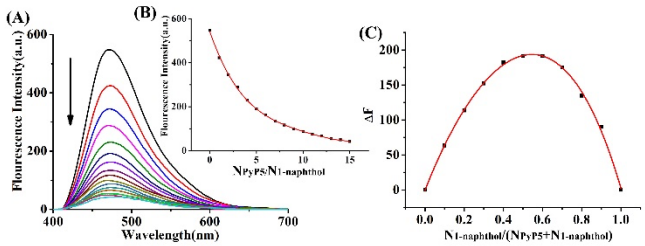

Figure 1. (A) Fluorescence spectra of 1-naphthol (20μM) with increasing amounts of PyP5 from 0, 20, 40, 60, 80, 100, 120, 140, 160, 180, 200, 220, 240, 260, 280 and 300 μM; (B) plots of $N_{PyP5}/N_{1\text{-naphthol}}$ *vs* fluorescence intensity of 1-naphthol in aqueous solution; (C) The Job's plot obtained by continuous variation of the mole fraction of 1-naphthol and PyP5 from aqueous solutions.

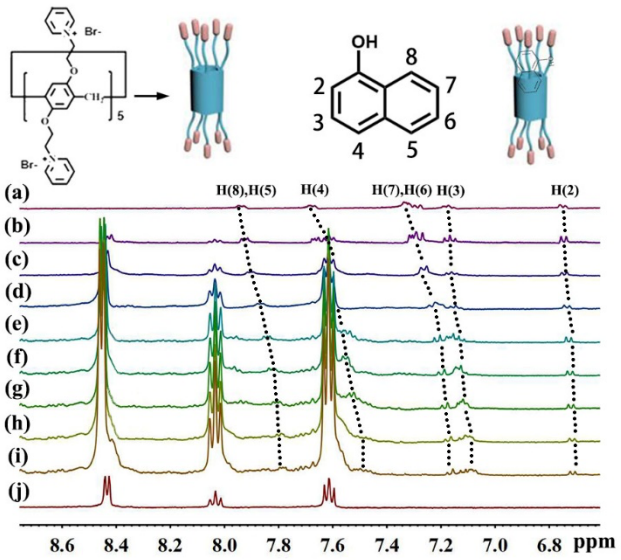

Figure 2. (A) 1-Naphthol spectrum and on addition of (b) 0.12, (c) 0.46, (d) 0.68, (e) 1.16, (f) 1.40, (g) 1.52, (h) 1.65, (i) 1.87 equivalents of PyP5 and (j) PyP5 ^{1}H NMR titration spectrum.

Figures 1A and B show that 1-naphthol (20μM) displays strong fluorescence with a maximum emission at 470 nm in solution. However, the titration florescence spectra of 1-naphthol decreased on increasing the amount of PyP5, which revealed the emergence of a robust supramolecular complex. The extinguishing of the fluorescence is attributed to the electron transfer between PyP5 and the electron-rich 1-naphthol. Moreover, using the Job's plot method, as shown in Figure 1C, it was observed that the maximum peak appeared at a mole fraction of 0.5, which corresponds to a 1:1 binding stoichiometry for PyP5 to 1-naphthol. As shown in Figure S1, the UV- vis spectra were obtained using aqueous solutions containing a fixed concentration of PyP5 (2.0×10^{-5} mol/L) and variable concentrations of 1-naphthol. On gradually increasing the 1-naphthol concentration in the PyP5 solution, the absorption band of the PyP5 exhibits a progressively higher absorbance due to the formation of the host - guest complex PyP5@1-naphthol. This is compatible with the results acquired from the fluorescence spectra.

^{1}H NMR titration spectra were obtained for a fixed amount of 1-naphthol in neutral aqueous solution and on gradual addition of PyP5 (Figure 2). Upon continuous addition of PyP5, only 1-naphthol proton resonances changed, suggesting that 1-naphthol had a high exchange ratio for binding and unbinding on the NMR time scale. As shown in Figure 2, when PyP5 was added to the 1-naphthol solution, the protons H2, H3, H4, H5, H6, H7, and H8 all underwent a clear upfield shift (H2= 0.05; H3= 0.08; H4= 0.22; H5 = 0.16; H6 = 0.23; H7 = 0.11; H8 = 0.16 ppm), indicating that 1-naphthol has entered the cavity of PyP5.

Response of the 1-naphthol@PyP5 inclusion complex to different metal ions (M^{n+})

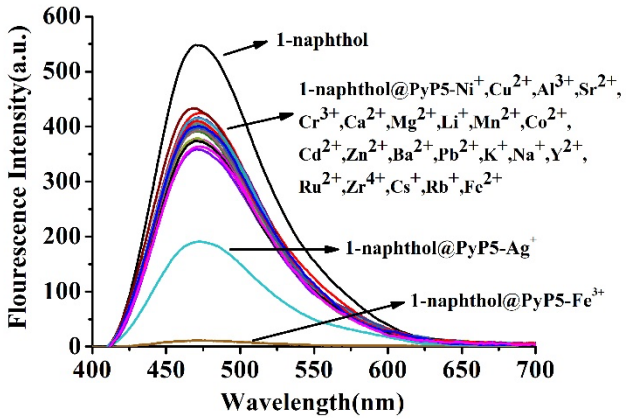

Figure 3. Fluorescence spectral response of metal cation (50 times) to 1-naphthol@PyP5 (20 μM).

The fluorescence properties of PyP5@1-naphthol indicated that it should be suitable for the rapid detection of metal ions. Thus, the PyP5@1-naphthol could be used as a probe to recognize metal cations. Herein, we investigated the fluorescence response of the PyP5@1-naphthol (1:1, 20μM) with metal cations (1mM).

After adding the metal ions to the supramolecular fluorescent probe PyP5@1-naphthol (20 μM), it was found that Fe^{3+} causes the fluorescence of the supramolecular fluorescent probe to be quenched, and a white precipitate is observed under natural light, whilst Ag^{+} also causes fluorescence decreased (as shown in Figure 3). The fluorescence intensity of the molecular fluorescent probe is reduced, and red-brown precipitation is observed under natural light (as shown in Figure 4). The addition of other metal

ions resulted in no obvious change in the fluorescence intensity of the probe. On placing the solution under 365 nm ultraviolet light, adding Fe^{3+} makes the PyP5@1-naphthol probe solution non-

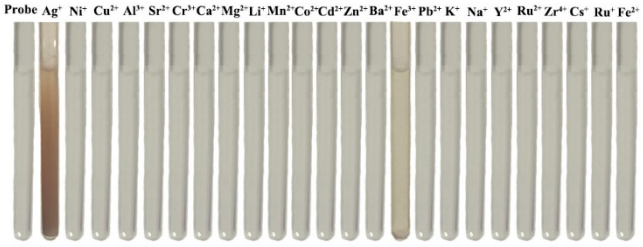

fluorescent, and adding Ag^{+} makes the fluorescence of probe solution significantly reduced (as shown in Figure 5).

Figure 4. 1-naphthol@PyP5 probe and the color change diagram of the probe-metal ion solutions under natural light.

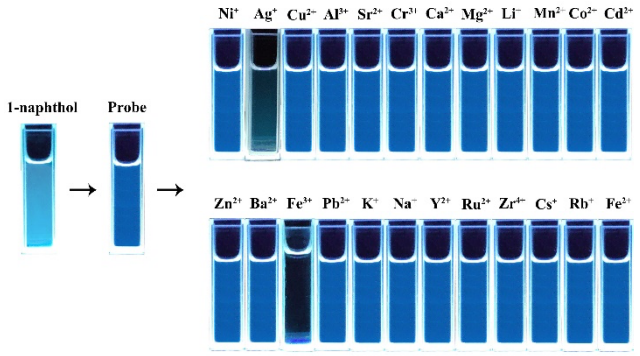

Figure 5. The color change diagram of 1-naphthol, 1-naphthol@PyP5 probe and probe-metal ion solution under 365nm UV lamp.

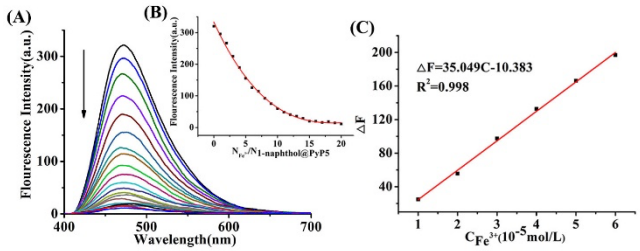

Figure 6. (A) Fluorescence spectra of Fe^{3+} titration probe 1-naphthol@PyP5; (B) The relationship between fluorescence emission and $N_{PyP5@1\text{-naphthol}}/N_{Fe^{3+}}$; (C). Linear fitting curve of the fluorescence intensity of 1-naphthol@PyP5 titration with different concentrations of Fe^{3+}.

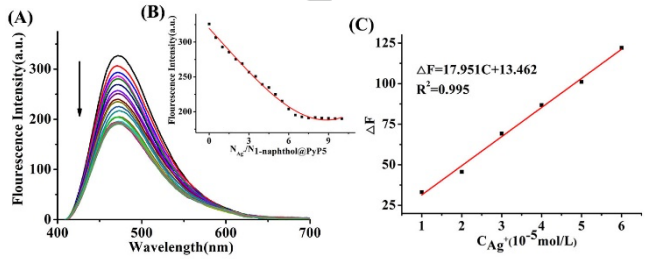

Figure 7. (A) Fluorescence spectra of Ag^{+} titration probe 1-naphthol@PyP5; (B) the relationship between fluorescence emission and $N_{PyP5@1\text{-naphthol}}/N_{Ag^{+}}$; (C) Ag^{+} counter-probe 1-naphthol at different concentrations and linear fitting curve graph of the fluorescence intensity change for the @PyP5 titration.

The concentration of the fluorescent probe PyP5@1-naphthol was fixed at 2.0×10^{-5} mol/L, and different volume fractions of Fe^{3+} ions were added to the fluorescent probe standard solution, and in Figure 6, it can be seen that the fluorescence intensity gradually decreases. Using the intensity reduction value as the ordinate, and the Fe^{3+} ion concentration as the abscissa, a calibration curve was drawn, and applying IUPAC regulations, the detection limit of the PyP5@1-naphthol probe for different amounts of Fe^{3+} ions was calculated. When the confidence level is 90%, K is 3, and the detection limit of Fe^{3+} is calculated to be 8.56×10^{-8} mol/L (Figure 6). The detection limit of Ag^{+} was determined by the same method as 1.67×10^{-7} mol/L (Figure 7).

In order to further study the mode of action of the metal ions Fe^{3+} and Ag^{+} with the probe PyP5@1-naphthol, we conducted an NMR specroscopic titration experiment with the metal ion and the probe PyP5@1-naphthol. The metal ion Fe^{3+} was gradually added to the quantitative probe PyP5@1-naphthol (1:1; 20μM), and the results showed that with the addition of Fe^{3+}, the host-guest proton peaks of the fluorescent probe 1-naphthol@PyP5 gradually disappeared, accompanied by a white precipitate. Eventually, the probe 1-naphthol@PyP5 was completely precipitated and the signals of the host-guest protons had completely disappeared (as shown in Figure S2). In a similar fashion, Ag^{+} ion was gradually added to the quantitative probe 1-naphthol@PyP5 (1:1; 20 μM) for ^{1}H NMR spectroscopic titration experiments. The results revealed that with the addition of Ag^{+}, the phenomenon is similar to that of Fe^{3+} (as shown in Figure S3). It is speculated that the luminescent Förster resonance energy transfer (FRET) might play a crucial role in the detection of these analytes. The UV-vis absorption spectra of Fe^{3+} exhibited a maximum overlap with the excitation spectrum of 1-naphthol between 240 nm and 330 nm, and the efficient absorption of Fe^{3+} at the excitation wavelength (293 nm) may hinder the absorption of 1-naphthol, resulting in the remarkable decrease or quenching of the luminescence compared with other ions. In the case of Ag^{+}, it may combine with Br^{-} from the PyP5 leading to AgBr precipitation.

Conclusion

In summary, the interaction of 1-naphthol with PyP5 was investigated using various techniques, and the results revealed a 1:1 host - guest inclusion complex, namely 1-naphthol@PyP5, exhibiting strong fluorescence emission. The complex was tested as a fluorescent probe for the detection of various metal cations. The results showed that the 1-naphthol@PyP5 inclusion complex exhibited unique responses to Ag^{+} cations, accompanied by a partial fluorescence quenching and reddish-brown precipitate appears; the 1-naphthol@PyP5 inclusion complex also exhibited unique responses to Fe^{3+} cations, accompanied by complete fluorescence quenching and the appearance of a white precipitate. The research results show that the probe PyP5@1-naphthol can

specifically detect Fe^{3+} and Ag^{+}, and has the advantages of high sensitivity and a low detection limit.

Experimental Section

Materials

1-naphthol and perchlorate were purchased from the Aladdin company, whilst all other reagents were of analytical reagent quality and were used without any further purification. PyP5 was synthesized according to the literature[57]. Doubly-distilled water was employed throughout.

Synthesis of PyP5

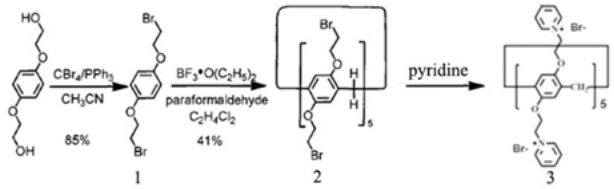

Figure 8. Synthetic route of PyP5.

While stirring at 0 °C, carbon tetrabromide (39.8 g, 120 mmol) was slowly added to the dissolved 1,4-bis(2-hydroxyethoxy)benzene (10.0 g, 50.4 mmol) and triphenylphosphine (31.5 g, 120 mmol) in 300 mL dried acetonitrile solution. The clear solution obtained after the reaction mixture was heated to room temperature under the protection of inert nitrogen was stirred for another 4 h. Then 200 mL of cold water was added to the reaction mixture to obtain a white solid. The white solid was collected by vacuum filtration, washed thoroughly with a 60:40 mixed solvent of V methanol: V water, and recrystallized from methanol to obtain white flake crystals. After vacuum drying, product **1** (13.8 g, 85%) was obtained.

Under the protection of nitrogen, product **1** (3.37 g, 11.5 mmol) and paraformaldehyde (0.349 g, 11.5 mmol) were dissolved in 200 mL of 1,2-dichloroethane solution. Then, boron trifluoride ether ($BF_3{\cdot}(OC_2H_5)_2$, 1.63 g, 11.5 mmol) was added as a catalyst, and the mixture was stirred at room temperature for 3 h to obtain a green solution. After filtration, the solid was placed on silica gel with a mixed solvent of petroleum ether/dichloromethane (1:2 v/v) as the eluent for column chromatography purification to obtain a white powder product **2** (1.6 g, 41%).

Product **2** (1.00 g, 0.595 mmol) and pyridine (1.88 g, 23.8 mmol) were added to 50 mL ethanol. The solution was stirred and heated to 80 ℃ and refluxed for 24 h. The solution was evaporated to obtain a solid, which was washed with ether solution. A white solid product **3** (1.28 g, 92%) was obtained, which is a PyP5 (Figure 1).

Measurement of absorption and fluorescence spectra

All UV/Visible spectra were recorded on an Agilent 8453 spectrophotometer (Agilent Technologies, Santa Clara, CA, USA), from solutions in 1 cm quartz cells. Fluorescence emission spectra were recorded on a VARIAN Cary Eclipse spectrofluorometer (Varian, Inc., Palo Alto, CA, USA). Fluorescence spectra were obtained by excitation at 293 nm with 5 nm emission and excitation bandwidths. Stock solutions of PyP5 (1.00×10^{-3} mol/L), 1-naphthol (1.00×10^{-3} mol/L) and M^{n+} (2.00×10^{-2} mol/L) were prepared in doubly-distilled water. Working solutions were prepared by diluting stock solutions to the required concentrations. Aqueous solutions of 1-naphthol (2.00×10^{-5} mol/L) were prepared by diluting the stock solutions. For absorption and fluorescence spectra, increasing concentrations ($0 - 30.0\times10^{-5}$ mol/L) of PyP5 solution were added to 1-naphthol. The excitation and maximum emission wavelengths (λex/λem) were 293 nm/ and 470 nm for the 1-naphthol/PyP5 complex, with 5 nm emission and excitation bandwidths. Aqueous solutions of the 1-naphthol/PyP5 complex (1-naphthol: 2.00×10^{-5} mol/L) were prepared for characterization by fluorescence emission spectroscopy. To obtain fluorescence spectra, known quantities of metal ion solutions were added to the 1-naphthol/PyP5 complex. Fluorescence spectra were obtained by excitation at 293 nm with 5 nm emission and excitation bandwidths at room temperature. The maximum emission wavelength was λem=470 nm for the 1-naphthol/PyP5 complex. For each experiment, three replicate measurements were made.

^{1}H NMR measurements

The ^{1}H NMR spectra were recorded using a JEOL JNM-ECZ400s spectrometer at 25°C. D_2O was used as a field-frequency lock and the observed chemical shifts are reported in parts per million (ppm) relative to that of the internal tetramethylsilane (TMS) standard (0.0 ppm).

Detection Limit

The detection limit of Fe^{3+} and Ag^{+} was determined by fluorescence titration. Fluorescence emission spectra of a series of mixture of certain amount of 1-naphthol@PyP5 and Fe^{3+} and Ag^{+} were recorded at room temperature. The calculation technique used for the DLs was based on the standard derivation of 10 measurements without the guest molecule (σ) and the slope of the linear calibration curve (K) based on the formula DLs

$$\sigma = \sqrt{\frac{1}{n-1}\sum_{i=1}^{n}(x_i - \bar{x})^2}$$

= 3σ/K. The standard deviation of 10 measurements without the guest molecule could be determined based on the following relationship:

where n is the number of measurements (n=11).

Acknowledgements

This work was supported by the National Natural Science Foundation of China (No. 21861011), the Innovation Program for High-level Talents of Guizhou Province (No. 2016-5657). CR thanks the EPSRC for an Overseas Travel Grant (EP/R023816/1).

Keywords: pillar[5]arene • 1-naphthol • host-guest • fluorescence probe • metal cations

[1] Y. Z. Chi, H. N. Li, L. Fan, C. Y. Du, J. L. Zhang, H. S, Guan, P. Wang, R. Li, *Carbohyd. Polym.* **2021**, 272, 118508.
[2] B. Li, J. Zhou, F. Y. Bai, Y. H. Xing, *Dyes. Pigments.* **2020**, 172, 107862.
[3] H. Y. Wang, M. Y. Fu, H. L. Zhai, Q. Y. Zhu, J. Dai, *Inorg. Chem.* **2021**, 60, 12255-12262.
[4] W. Zhou, P. T. Wu, L. Zhang, D. L. Zhu, X. N. Zhao, Y. H. Cai, *J. Hazard. Mater.* **2021**, 421, 126721.
[5] N. Zhang, Y. H. Xing, F. Y. Bai, *Cryst. Growth Des.* **2020**, 20, 1838−1848.
[6] Q. L. Guan, C. Han, F. Y. Bai, J. Liu, Y. H. Xing, Z. Shi, L. X. Sun, *Sensor. Actuat. B-Chem.* **2020**, 325, 128767.

[7] Q. L. Guan, Y. Sun, R. Huo, Y. Xin, F. Y. Bai, Y. H. Xing, L. X. Sun, *Inorg. Chem.* **2021**, 60, 2829-2838.

[8] Y. Xiao, B. Li, Z. X. You, Y. H. Xing, F. Y. Bai, L. X. Sun, Z. Shi, *J. Mater. Chem. C*. **2021**, 9, 3193-3203.

[9] Y. Zhao, N. Zhang, Y. Wang, F. Y. Bai, Y. H. Xing, L. X. Sun, *Inorg. Chem. Front.* **2021**, 8, 1736-1746.

[10] N. Du, J. Song, S. Li, Y. X. Chi, F. Y. Bai, Y. H. Xing, *ACS Appl. Mater. Inter*. **2016**, 8, 28718-28726.

[11] X. Liang, Z. J. Ni, L. M. Zhao, B. Ge, H. Zhao, W. Z. Li, *Microchem. J.* **2021**, 170, 106663.

[12] H. R. Lin, G. C. Chen, H. M. Zhao, Y. Q. Cao, *J. Environ. Manage.* **2021**, 298, 113458.

[13] N. T. Yang, Z. L. Ren, C. G. Yang, P. Wu, G. F. Zeng, *Fuel.* **2021**, 305, 121624.

[14] X. Li, Y. Yuan, Y. Huang, *J. Clean. Prod.* **2021**, 317, 128499.

[15] C. Zhou, L. Zhu, L. Deng, H. J. Zhang, H. X. Zeng, Z. Shi, *Sep. Purif. Technol.* **2021**, 276, 119404.

[16] L. Y. Ma, S. S. Huang, P. Y. Wu, J. M. Xiong, H. M. Wang, H. H. Liao, X. D. Liu, *Sci. Total. Environ.* **2021**, 798, 149186.

[17] C. Liu, H. Yi, B. Q. Yang, F. F. Jia, S. X. Song, *Appl. Surf. Sci.* **2021**, 566, 150674.

[18] X. D. Zhao, L. Pei, H. H. Fan, Y. Z. Zhang, B. S. Liu, X. L. Gao, Y. H. Wei, *J. Solid. State. Chem.* **2021**, 302, 122460.

[19] T. J. Jayeoye, J. Ma, T. Rujiralai, *J. Environ. Chem. Eng.* **2021**, 9, 105770.

[20] C. B. Liu, X. J. Wei, S. B. Hao, B. Y. Zong, X. Y. Chen, Z. Li, S. Mao, *Anal. Chem.* **2021,** 93, 8010-8018.

[21] H. X. Li, M. H. Chen, R. Luo, W. P. Peng, X. Q. Gong, J. Chang, *Colloid. Surface. B.* **2021**, 202, 111686.

[22] J. Y. Zhao, G. X. Liu, Y. X. Lu, Y. W. Guan, Y. Y. Liu, *Sensor. Actuat. B-Chem.* **2021**, 330, 129382.

[23] Q. Li, Z. L. Bai, X. J. Xi, Z. W. Guo, C. Liu, X. R. Liu, X. Y. Zhao, Z. Y. Li, Y. Cheng, Y. Wei, *Spectrochim. Acta. A.* **2021**, 248, 119208.

[24] A. Pundi, C. J. Chang, Y. S. Chen, J. K. Chen, J. M. Yeh, C. S. Zhuang, M. C. Lee, *Spectrochim. Acta. A.* **2021**, 247, 119075.

[25] Y. Y. Tian, Y. C. Chen, M. Chen, Z. L. Song, B. Xiong, X. B. Zhang, *Talanta.* **2021**, 221, 121627.

[26] J. Q. Guo, S. Ye, H. Li, J. Song, J. L. Qu, *Dyes. Pigments.* **2020**, 183, 108723.

[27] Y. F. Xie, Y. J. Jiang, H. Y. Zou, J. Wang, C. Z. Huang, *Talanta*. **2020**, 220, 121430.

[28] L. Wang, C. Z. Zhang, H. He, H. X. Zhu, W. Guo, S. L. Zhou, S. F. Wang, J. R. Zhao, J. Zhang, *Int. J. Biol. Macromol*. **2020**, 163, 593-602.

[29] A. R. Hughes, M. Liu, S. Paul, A. I. Cooper, F. Blanc, *J. Phys. Chem. C.* **2021**, 125, 13370-13381.

[30] J. B. Yao, W. H. Wu, C. Xiao, D. Su, Z. H. Zhong, T. Mori, C. Yang, *Nat. Commun.* **2021**, 12, 2600.

[31] Z. Wang, T. Chen, H. Liu, X. L. Zhao, W. B. Hu, H. Yang, Y. A. Liu, K. Wen, *J. Org. Chem*. **2021**, 86, 6467-6477.

[32] D. Kaizerman-Kane, M. Hadar, R. Joseph, D. Logviniuk, Y. Zafrani, M. Fridman, Y. Cohen, *Acs. Infect. Dis*. **2021**, 7, 579-585.

[33] Y. Cai, X. Yan, S. Y. Wang, Z. W. Zhu, M. P. Cen, C. J. Ou, Q. Zhao, Q. Yan, J. Wang, Y. Yao, *Inorg. Chem.* **2021**, 60, 2883-2887.

[34] Y. Cai, Z. C. Zhang, Y. Ding, L. P. Hu, J. Wang, T. T. Chen, Y. Yao, *Chinese. Chem. Lett.* **2021**, 32, 1267-1279.

[35] B. Liu, X. J. Lu, X. K. Liao, H. Zou, J. T. Tao, C. Y. Ni, J. Q. Pan, C. R. Li, Y. Y. Zheng, *Appl. Surf. Sci.* **2021**, 566, 150739.

[36] X. Q. Tian, M. Z. Zuo, P. B. Niu, K. Velmurugan, K. Wang, Y. Zhao, L. Y. Wang, X. Y. Hu, *ACS. Appl. Mater. Inter.* **2021**, 13, 37466-37474.

[37] J. J. Cao, H. T. Z. Zhu, L. Q. Shangguan, Y. Z. Liu, P. R. Liu, Q. Li, Y. T. Wu, F. H. Huang, *Polym. Chem-UK*. **2021**, 12, 3517-3521.

[38] S. W. Guo, Q. X. Huang, Y. Chen, J. W. Wei, J. Zheng, L. Y. Wang, Y. T. Wang, R. B. Wang, *Angew. Chem. Int. Edit.* **2021**, 60, 618-623.

[39] M. Li, B. Hua, F. H. Huang, *Org. Chem. Front.* **2021**, 8, 3675-3680.

[40] M. B. Wang, Q. Li, E. R. Li, J. Y. Liu, J. Zhou, F. H. Huang, *Angew. Chem. Int. Edit.* **2021**, 60, 8115-8120.

[41] X. P. Tan, Y. Wu, S. Yu, T. Y. Zhang, H. X. Tian, S. H. He, A. N. Zhao, Y. W. Chen, Q. Gou, *Talanta*. **2019**, 195, 472-479.

[42] G. F. Zhao, L. Yang, S. L. Wu, H. Zhao, E. Tang, C. P. Li, *Biosens. Bioelectron*. **2017**, 91, 863-869.

[43] X. W. Mao, T. Liu, J. H. Bi, L. Luo, D. M. Tian, H. B. Li, *Chem. Commun.* **2016**, 52, 4385-4388.

[44] F. Zhang, X. L. Cao, D. M. Tian, H. B. Li, *Chinese. J. Chem*. **2015**, 33, 368-372.

[45] P. Wang, Y. Yao, M. Xue, *Chem. Commun*. **2014**, 50, 5064-5067.

[46] M. Cheng, G. Li, W. W. Xu, H. N. Qu, X. W. Mao, H. B. Li, *Dyes. Pigments.* **2021**, 194, 109646.

[47] M. Z. Zuo, W. R. Qian, M. Hao, K. Y. Wang, X. Y. Hu, L. Y. Wang, *Chinese. Chem. Lett.* **2021**, 32, 1381-1384.

[48] L. Shao, J. F. Sun, B. Hua, F. H. Huang, *Chem. Commun.* **2018**, 54, 4866-4869.

[49] W. R. Qian, M. Z. Zuo, G. P. Sun, Y. Chen, T. T. Han, X. Y. Hu, R. B. Wang, L. Y. Wang, *Chem. Commun.* **2020**, 56, 7301-7304.

[50] L. L. Yang, R. Z. Gong, G. I. N. Waterhouse, J. Dong, J. Xu, *Environ. Sci. Pollut. R.* **2021**, 28, 31185-31194.

[51] J. W. Huang, D. Chen, X. K. Kong, S. R. Wu, K. Chen, J. D. Jiang, *Appl. Environ. Microb.* **2021**, 87, e00170-21.

[52] W. Ming, F. Chen, X. J. Hu, Z. Z. Zhang, S. Z. Chang, R. S. Chen, B. Z. Tian, J. L. Zhang, *Tetrahedron*. **2020,** 76, 131420.

[53] Y. Chen, B. B. Sun, R. R. Wang, C. H. Shi, M. Cheng, J. L. Jiang, C. Lin, L. Y. Wang, *Org. Lett.* **2021**, 23, 7423-7427.

[54] L. Barbera, D. Franco, L. M. De Plano, G. Gattuso, S. P. P. Guglielmino, G. Lentini, N. Manganaro, N. Marino, S. Pappalardo, M. F. Parisi, F. Puntoriero, I. Pisagatti, A. Notti, *Org. Biomol. Chem*. **2017**, 15, 3192-3195.

[55] S. Wang, Z. Q. Xu, T. T. Wang, X. Liu, Y. M. Lin, Y. Z. Shen, C. Lin, L. Y. Wang, *J. Photoch. Photobio. A*. **2018**, 355, 60-66.

[56] Q. Wang, X. Y. Bian, X. L. Chen, Y. Han, C. G. Yan, J. Mol. Struct. 2020, 1210, 128004.

[57] Y. J. Ma, X. F. Ji, F. Xiang, X. D. Chi, C. Y. Han, J. M. He, Z. Abliz, W. X. Chen, F. H. Huang, *Chem. Commun.* **2011**, 47, 12340-12342.

Entry for the Table of Contents